

Article

Oxidative-Stress-Related Alterations in Metabolic Panel, Red Blood Cell Indices, and Erythrocyte Morphology in a Type 1 Diabetic Rat Model

Zita Szalai ¹, Anikó Magyariné Berkó ¹, Nikolett Bódi ¹, Edit Hermeszt ² , Ágnes Ferencz ²
and Mária Bagyánszki ^{1,*} 

¹ Department of Physiology, Anatomy and Neuroscience, Faculty of Science and Informatics, University of Szeged, 6726 Szeged, Hungary; zszalai@bio.u-szeged.hu (Z.S.); berko@bio.u-szeged.hu (A.M.B.); bodi.nikolett@bio.u-szeged.hu (N.B.)

² Department of Biochemistry and Molecular Biology, Faculty of Science and Informatics, University of Szeged, 6726 Szeged, Hungary; hermeszt@bio.u-szeged.hu (E.H.); agnes.ferencz@bio.u-szeged.hu (Á.F.)

* Correspondence: bmarcsi@bio.u-szeged.hu; Tel.: +36-62-544-143

Abstract: Diabetes mellitus is often associated with vascular complications in which hyperglycemia-induced oxidative stress may be the cause of the impaired vessels and circulating blood cells. The aim of this study was to follow the hyperglycemia-related metabolic and morphological changes in blood and urine samples of Wistar rats. Animals were divided into streptozotocin-induced diabetic (acute and chronic), insulin-treated diabetic, reversed diabetic, and control groups. In chronic diabetic rats, decreases in albumin, total protein, and antioxidant glutation concentration were measured, while glutamic-pyruvic transaminase, alkaline phosphatase, red blood cell (RBC) count, hematocrit, and hemoglobin levels were increased. Moreover, an increased level of the phenotypic variants was detected in the RBC population of the diabetic animals. In conclusion, we verified the sensitivity of RBCs to long-lasting hyperglycemia, and to insulin deficiency, which were both accompanied with an increased level of RBC-derived parameters and the presence of eccentrocytes, hemolyzed RBCs, and codocytes. Moreover, our results show that the response of the RBC glutation system to oxidative stress depends on the duration of hyperglycemia, and that the short-term activation of this defense system is exhausted in a long-lasting oxidative environment. Insulin therapy was effective in the case of most parameters, which clearly emphasizes the importance of maintaining blood glucose at physiological level.

Keywords: hyperglycemia; streptozotocin-diabetic rats; insulin replacement; routine blood test; red blood cell morphology; glutathione; oxidative stress



Citation: Szalai, Z.; Berkó, A.M.; Bódi, N.; Hermeszt, E.; Ferencz, Á.; Bagyánszki, M. Oxidative-Stress-Related Alterations in Metabolic Panel, Red Blood Cell Indices, and Erythrocyte Morphology in a Type 1 Diabetic Rat Model. *Appl. Sci.* **2023**, *13*, 9920. <https://doi.org/10.3390/app13179920>

Academic Editor: Marco G. Alves

Received: 7 July 2023

Revised: 29 August 2023

Accepted: 30 August 2023

Published: 1 September 2023



Copyright: © 2023 by the authors. Licensee MDPI, Basel, Switzerland. This article is an open access article distributed under the terms and conditions of the Creative Commons Attribution (CC BY) license (<https://creativecommons.org/licenses/by/4.0/>).

1. Introduction

Diabetes mellitus is a risk factor for the development of several macrovascular or microvascular complications such as coronary heart disease, ischemic strokes, retinopathy, nephropathy, and neuropathy [1,2]. The underlying mechanisms behind vascular complications are multifactorial and complex. Red blood cells (RBCs) are implicated in the pathomechanism of vascular disturbances [3]. They are highly sensitive to most pathological conditions, such as hyperglycemia, because they lose their organelles when mature and only preserve a few metabolic pathways [4]. Moreover, in a hyperglycemic environment, glucose concentration increases in the RBC cytosol because of passive glucose influx via the insulin-independent glucose transporter, which leads to non-enzymatic glycosylation of structural and functional proteins and the formation of advanced glycation end products [5,6]. The glycosylation of RBC membrane components causes irreversible cross-linking of cytoskeletal proteins, thereby reducing membrane fluidity, which leads to decreased relative lateral fluidity of proteins and lipids in the membrane structure.

The changed fluidity of diabetic RBCs results in the decreased deformability of cells and increases their aggregation. The stiffened and rigid membrane and clumping of RBCs make it difficult for them to pass through the microvessels, causing microvascular complications [7,8]. A well-known glycosylated protein is the glycosylated hemoglobin A1c (HbA1c). The analysis of HbA1c in clinical tests of diabetic patients is routinely used to determine long-lasting blood glucose exposure [9]. In addition, HbA1c was found to be an independent cardiovascular risk factor. The glycosylated Hb is more susceptible to degradation, which leads to the enhanced fragility of RBCs, which in turn release higher quantities of free heme and iron, leading to oxidative stress. Moreover, glycosylated Hb may contribute to endothelial inflammation and vascular dysfunction [10]. Earlier studies demonstrated that diabetic patients may have other alterations in various hematological parameters, including RBC indices such as RBC count, mean corpuscular volume (MCV), or red blood cell volume distribution width (RDW) [5]. In addition, the higher proportion of morphologically altered RBCs in diabetes is a known consequence of this pathological condition; however, only a few studies have focused on quantification of different types of abnormally shaped RBCs in diabetic and insulin-treated diabetic rats using blood smears [8,11,12].

A disturbance in the balance of antioxidants and oxidants leads to oxidative stress. Oxidative stress is an important deleterious agent in several pathological conditions, such as chronic hyperglycemia, inflammation, or aging. Although RBCs do not have mitochondria, which are the main source of reactive oxygen and nitrogen species (RONS) in most cells, RONS are produced continuously in RBCs because of the heme iron content and the high oxygen tension in arteries. The elevated production of advanced glycation end products in chronic hyperglycemia is a triggering factor due to the glyco-oxidative stress. The antioxidant defense system, which scavenges and detoxifies RONS, consists of enzymatic and non-enzymatic pathways, such as superoxide dismutase, catalase, glutathione peroxidase (GSHPx), glutathione reductase (GR)-dependent regeneration of glutathione and NADH-methemoglobin reductase or reduced glutathione (GSH), uric acid, and vitamins A, C, and E. The main non-enzymatic antioxidant in RBCs is the tripeptide GSH, which exists either in reduced or oxidized (GSSG) form via the reversible oxidation of its active thiol. The reactions are facilitated by GSHPx and GR. The ratio of GSH/GSSG indicates the redox potential of the cell. Moreover, GSH has multiple protective roles in defense mechanisms. It can directly scavenge free radicals or play a role as a substrate during the detoxification of hydrogen peroxide and lipid hydroperoxides catalyzed by GSHPx and glutathione-S-transferase [13,14].

The aim of this study was to follow the hyperglycemia-related metabolic and morphological changes in blood and urine samples of Wistar rats, focusing on the possible oxidative stress-mediated changes.

2. Materials and Methods

2.1. Animal Models

Adult male Wistar rats (CrI:WI BR; Toxi-Coop Zrt., Balatonfüred, Hungary) kept on a 12/12 h day/night cycle, fed standard laboratory chow (Farmer-Mix Kft., Zsámbék, Hungary), and with free access to drinking water, were used throughout the 1-week acclimatization period and the experiments. The protocol was designed to minimize pain or discomfort to the animals. In all procedures involving experimental animals, the principles of the National Institutes of Health (Bethesda, MD, USA) guidelines and the EU directive 2010/63/EU (<https://eur-lex.europa.eu/LexUriServ/LexUriServ.do?uri=OJ:L:2010:276:0033:0079:en:PDF>, accessed on 6 July 2023) for the protection of animals used for scientific purposes were strictly followed, and all the experiments were approved by the National Scientific Ethical Committee on Animal Experimentation (National Competent Authority), with the license number XX./1636/2019.

For the acute hyperglycemic experiments, before STZ injection the rats (280–320 g, 12-week-old) were divided randomly into two groups: STZ-induced 5-day diabetics (acute diabetics, $n = 7$), and age-matched controls ($n = 6$). The controls were treated with vehicle,

while diabetes was induced by a single intraperitoneal injection of STZ (Sigma-Aldrich, Budapest, Hungary) at 60 mg/kg, as described previously [15,16]. The animals were considered diabetic if the non-fasting blood glucose concentration was higher than 18 mmol/L. The blood glucose level and weight of each animal were measured daily.

For the chronic hyperglycemic experiments, before STZ injection the rats (200–260 g, 7–8-week-old) were divided randomly into four groups: STZ-induced 10-week diabetics (chronic diabetics; $n = 14$), insulin-treated STZ-induced diabetics (insulin-treated diabetics; $n = 13$), reverted STZ-induced diabetics (reverted diabetics; $n = 4$), and age-matched controls ($n = 20$). The controls were treated with vehicle, while diabetes was induced by a single intraperitoneal injection of STZ, as previously mentioned. The animals were considered diabetic if the non-fasting blood glucose concentration was higher than 18 mmol/L. From this time on, one group of hyperglycemic rats received a subcutaneous injection of insulin (Humulin M3, Eli Lilly Nederland, Utrecht, The Netherlands) each morning (3 IU) and afternoon (3 IU). The rats of the chronic diabetic group were considered to be reverted diabetic if the non-fasting blood glucose concentration decreased and stayed under 18 mmol/L during the ten weeks. Equivalent volumes of saline were given subcutaneously to the diabetic, the reverted diabetic, and the control rats. The blood glucose level and weight of each animal were measured weekly.

2.2. Determination of Metabolic Panel and Complete Blood Count

After both 5 days and 10 weeks of STZ treatment, each rat was placed in a metabolic cage for urine collection. Carbamide and glucose levels of urine samples were determined with BiOLis 24i (Tokyo Boeki Machinery Ltd., Tokyo, Japan). The semiquantitative measurements of urine specific gravity, pH, leukocytes, nitrite, and ketones were performed by urine test strips (Arkray Ltd., Stokenchurch, UK).

Following this, on the next day, the blood samples were collected from the tail vein of each animal (BD Vacutainer SST II Advance serum tubes and BD Vacutainer K2E ethylenediaminetetraacetic acid (EDTA) 7.2 mg tubes, BD, Plymouth, UK).

Serum samples for clinical chemistry were left to clot at room temperature for 30 min before being centrifuged at 3200 rpm for 10 min at 20 °C. All parameters of clinical chemistry were measured from serum samples, except HbA1c, using the multi-function automatic analyzer system (BiOLis 24i). The level of HbA1c was determined from EDTA-containing blood samples on the BiOLis 24i.

The complete blood count and the derived parameters were determined from EDTA-containing blood samples using an ADVIA 120 hematology analyzer in CBC/Diff mode (Bayer Diagnostics, Tarrytown, NY, USA).

2.3. Determination of Diameter and Morphology of Red Blood Cells

Smears were made from whole blood immediately after sampling. Whole blood was diluted with a few drops of physiological saline (0.9%) when necessary. Blood smears were heat fixed to the slides (150 °C, 15 min) and kept at 4 °C until use.

Smears were fixed in methanol for 10 min and stained with hematoxylin-eosin (Leica Autostainer XL, Leica Biosystems, Deer Park, IL, USA). The stained smears were visualized and photographed with a 100× immersion objective on a Zeiss Imager Z.2 fluorescent microscope equipped with an AxioCam ICc 5 (Zeiss, Jena, Germany). Each RBC on 60 fields of view per group was evaluated for diameter and qualitative abnormalities, including echinocyte, acanthocyte, ovalocyte, dacrocyte, schistocyte, eccentrocyte, hemolyzed cell, or codocyte (Table 1) [17–19]. ImageJ 1.53t was used to quantify the erythrocyte diameter.

Table 1. The definition of the morphological abnormalities of red blood cells.

Morphological Types of RBCs	Definitions of Morphological Abnormalities
echinocytes	RBCs have regularly distributed, equally sized, rounded projections on their surface [18]
acanthocytes	RBCs have irregularly distributed, variably sized, pointy projections on their surface [17,18]
ovalocytes	RBCs have oval shape [18]
dacrocytes	RBCs are tapered to a point at one end, resembling the classic artist's rendition of a drop of water [18]
schistocytes	RBCs appear to have been fragmented: they lack the usual circular shape [18]
eccentrocytes	RBCs are with a clear crescent-shaped area along one side of the periphery [19]
hemolyzed RBCs	RBCs that are destroyed with the release of intracellular material [17]
codocytes	RBCs have a central red area within the zone of central pallor [18]

(RBCs: red blood cells).

2.4. Tissue Handling

Five days or ten weeks after the onset of hyperglycemia, the animals were killed by cervical dislocation under chloral hydrate anesthesia (375 mg/kg i. p.). The pancreas of diabetic, reverted diabetic, insulin-treated diabetic, and control rats were dissected and rinsed in 0.05 M phosphate buffer (PB; pH 7.4). Samples were fixed in 4% paraformaldehyde and embedded in melted paraffin.

2.5. Fluorescent Immunohistochemistry

For double-labeling fluorescent immunohistochemistry, paraffin-embedded pancreas sections were immunostained with insulin and glucagon. Briefly, after blocking in PB containing 0.1% bovine serum albumin, 10% normal goat serum, and 0.3% Triton X-100, the samples were incubated overnight with anti-insulin (mouse; I2018, Sigma-Aldrich, Budapest, Hungary; final dilution 1:100) and anti-glucagon (rabbit, ab92517, Abcam, Cambridge, UK; final dilution 1:200) primary antibodies at 4 °C. After washing in tris (hydroxymethyl)aminomethane-buffered saline with 0.025% Triton X-100, sections were incubated with anti-mouse CyTM3 (Jackson ImmunoResearch Laboratories, Inc., West Grove, PA, USA; final dilution 1:200) and anti-rabbit Alexa Fluor 488 (Life Technologies Corporation, Molecular Probes, Inc., Waltham, MA, USA; final dilution 1:200) secondary antibodies for 1 h at room temperature. Negative controls were performed by omitting the primary antibody when no immunoreactivity was observed. Paraffin sections were mounted on slides in FluoroshieldTM with DAPI histology mounting medium (Sigma-Aldrich, Budapest, Hungary) to label nuclei of cells, which were observed and photographed with a Zeiss Imager Z.2 fluorescent microscope equipped with an AxioCam 506 mono camera (Zeiss, Jena, Germany).

2.6. Determination of Reduced and Oxidized Glutathione Contents of Red Blood Cells

Blood coagulation was inhibited with EDTA. The blood samples were centrifuged at 1000 r.p.m. for 10 min at 20 °C, and the plasma and the buffy coat were removed. The phase of RBCs was washed twice with 2 volumes of isotonic saline solution at pH 7.4. The samples were stored at −80 °C until processing.

The RBCs were hemolyzed by the addition of distilled water at a ratio of 1:9. The aliquots of the hemolysates were used directly for GSH and protein analysis.

The quantity of protein was determined with Folin reagent (Merck Life Science Kft. Darmstadt, Germany), using bovine serum albumin (Sigma-Aldrich, Budapest, Hungary) as standard [20].

The concentrations of total and reduced GSH in the RBCs were measured as described by Sedlak and Lindsay [21]. GSSG was recycled in the presence of GR (EC 1.8.1.7) (Sigma-Aldrich, Budapest, Hungary) and NADPH (Sigma-Aldrich, Budapest, Hungary), and GSSG content was calculated from the difference in total GSH and reduced GSH values. The results are expressed in nmol/mg protein.

2.7. Statistical Analysis

Statistical analysis was performed with the Kruskal–Wallis test and Dunn’s multiple comparison test (chronic study) or unpaired *t*-test (acute study). All analyses were carried out using GraphPad Prism 6.0 (GraphPad Software, La Jolla, CA, USA). A probability of $p < 0.05$ was set as the level of significance. All data are expressed as means \pm SEM.

3. Results

3.1. Body Weight and Glycemic Characteristics in Diabetic Rats

According to the data shown in Tables 2 and 3, acute and chronic diabetic rats were characterized by significantly increased blood glucose level compared to the age-matched controls (acute: $p < 0.0001$; chronic: $p < 0.001$). Their urine glucose level ($p < 0.001$) and HbA1c level ($p < 0.01$) were markedly elevated. The insulin treatment during the ten weeks prevented an extremely high blood glucose level; however, it was still twice as high as in the controls. The urine glucose level and the HbA1c level of insulin-treated diabetic rats remained close to that of the control level. In the case of reverted diabetic rats, the blood glucose level was extremely elevated after the onset of diabetes (23.7 ± 1.2 mmol/L); however, during the ten-week experiment the rats recovered spontaneously and their blood glucose level dropped below 18 mmol/L, so 11.3 ± 1.2 mmol/L was measured on average. A slightly increased HbA1c was detected in reverted diabetic rats.

The body weight of the animals increased in all groups during both acute (Table 2) and chronic experiments (Table 3); however, this body weight gain was most prominent in the controls and the insulin-treated diabetics.

The Langerhans islets of pancreatic sections were visualized via double-labeling fluorescent immunohistochemistry against insulin (red) and glucagon (green; Figure 1). Weaker insulin immunostaining was found in both the acute and chronic diabetics, and in the insulin-treated diabetics, when compared to controls. Regenerated Langerhans islets were observed using immunostaining for insulin in the reverted diabetic group.

Table 2. Weight and glycemic characteristics of acute diabetic experiment.

		Controls (n = 6)	Acute Diabetics (n = 7)
Weight (g)	Initial	303.8 \pm 9.46	293.0 \pm 13.7
	Final	339.5 \pm 14.97	301.7 \pm 11.63
Blood glucose level (mmol/L)	Initial	5.5 \pm 0.2	5.9 \pm 0.3
	Final (average)	5.6 \pm 0.3	20.5 \pm 1.3 **** ^{oooo}
Urine glucose level (mmol/L)	Final	5.6 \pm 5.1	477.2 \pm 42.4 ^{ooo}
HbA1c (mmol/mol)	Final	12.0 \pm 1.2	21.8 \pm 1.3 ^{oo}
HbA1c (%)	Final	3.3 \pm 0.1	4.1 \pm 0.1 ^{oo}

Data are expressed as mean \pm SEM; **** $p < 0.0001$ vs. initial values; ^{oo} $p < 0.01$; ^{ooo} $p < 0.001$; ^{oooo} $p < 0.0001$ vs. final controls.

Table 3. Weight and glycemic characteristics of chronic diabetic rats.

		Controls (n = 20)	Chronic Diabetics (n = 14)	Insulin-Treated Diabetics (n = 13)	Reverted Diabetics (n = 4)
Weight (g)	Initial	222.1 ± 16.8	222.9 ± 17.2	230.2 ± 236	204.5 ± 5.9
	Final	460.3 ± 46.9 ***	354.0 ± 33.2 *	430.8 ± 41.0 ***	377.5 ± 26.1
Blood glucose level (mmol/L)	Initial	6.0 ± 0.2	5.7 ± 0.3	6.0 ± 0.2	6.7 ± 0.1
	Final (average)	5.7 ± 0.1	24.0 ± 0.7 *** ^{ooo}	11.8 ± 0.8 * ^{ooo}	a, 23.7 ± 1.2 ^{oo} b, 11.3 ± 1.2
Urine glucose level (mmol/L)	Final	0.31 ± 0.04	503.7 ± 12.3 ^{oooo}	0.39 ± 0.08 ⁺⁺⁺⁺	-
HbA1c (mmol/mol)	Final	21.0 ± 0.6	96.6 ± 9.5 ^{ooo}	23.8 ± 1.6 ⁺⁺	32.8 ± 5.1
HbA1c (%)	Final	4.1 ± 0.1	11.0 ± 0.9 ^{ooo}	4.3 ± 0.1 ⁺⁺	5.1 ± 0.5

a, value shows the average blood glucose levels of reverted diabetics measured before the rats recovered spontaneously; b, value shows the average blood glucose levels of reverted diabetics measured after the rats recovered spontaneously; Data are expressed as mean ± SEM; * $p < 0.05$; *** $p < 0.001$ vs. initial values; ^{oo} $p < 0.01$, ^{ooo} $p < 0.001$, ^{oooo} $p < 0.0001$ vs. final controls; ⁺⁺ $p < 0.01$; ⁺⁺⁺⁺ $p < 0.0001$ vs. final diabetics. (HbA1c: glycated hemoglobin A1c).

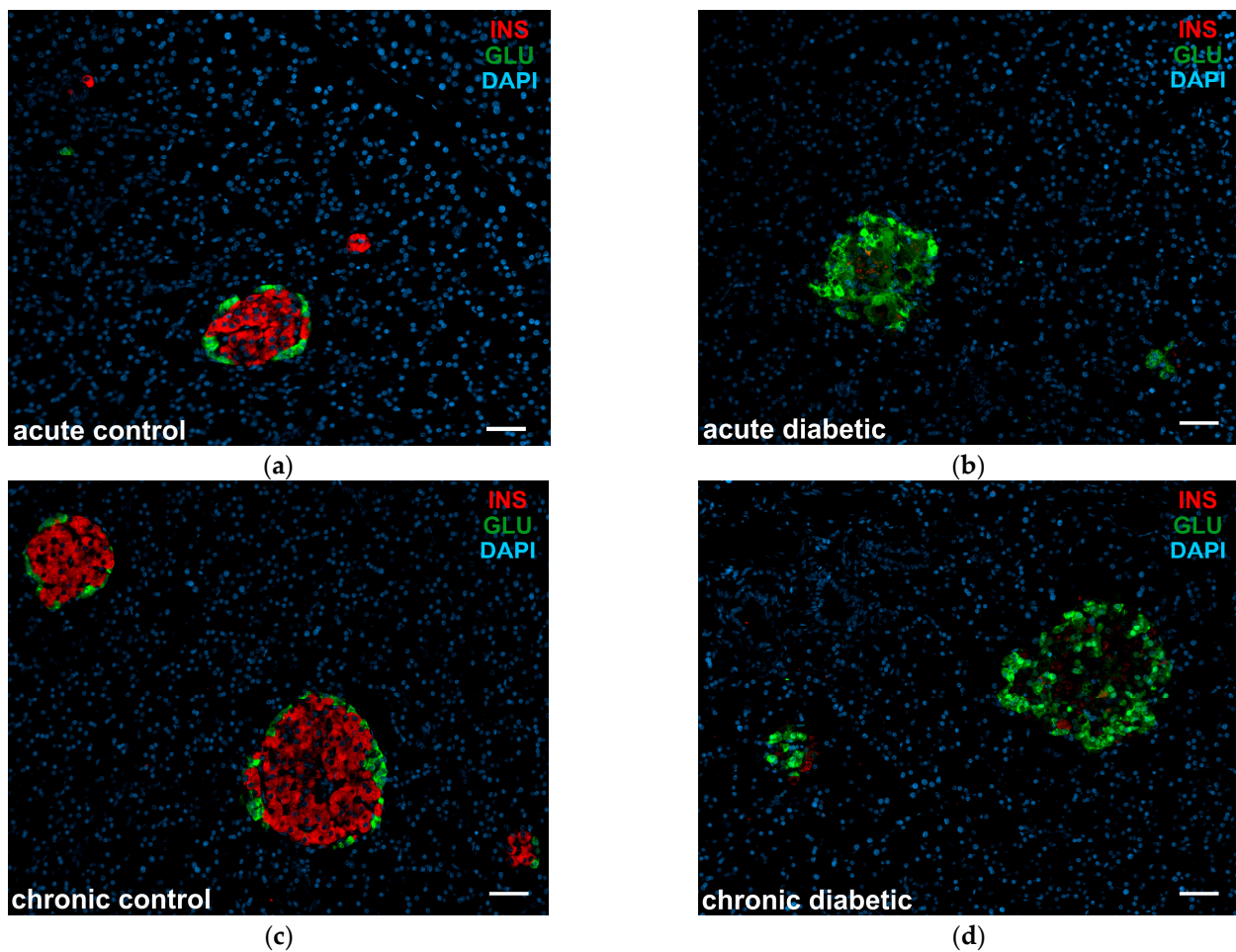


Figure 1. Cont.

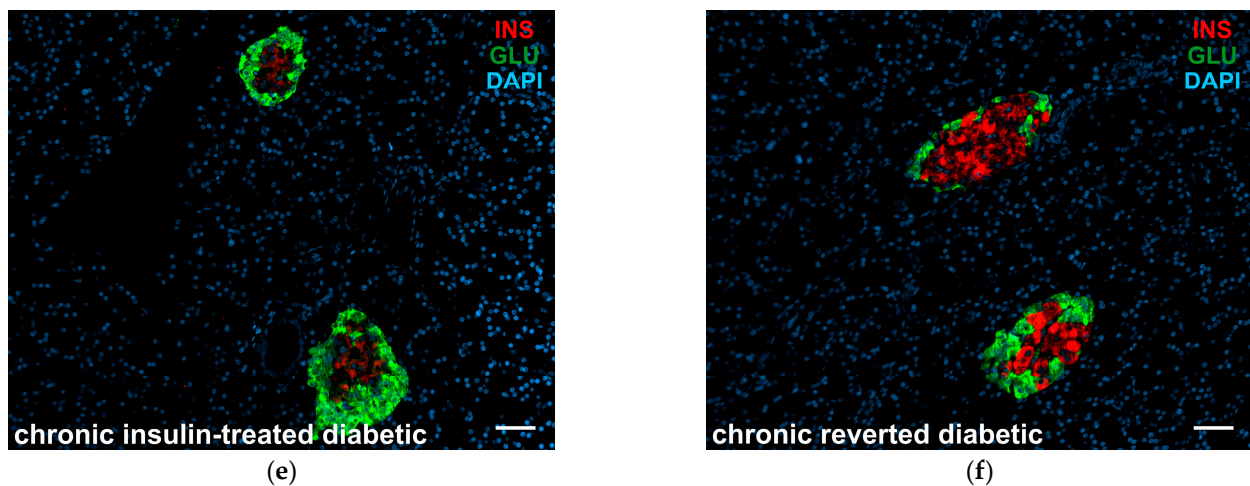


Figure 1. Representative fluorescent micrographs of paraffin-embedded pancreas sections from the different groups of (a,b) acute and (c–f) chronic experiments after insulin/glucagon double-labeling immunohistochemistry of Langerhans islets. DAPI was applied to label the nuclei of cells. The STZ treatment resulted in weaker staining for insulin in the diabetic and insulin-treated diabetic pancreatic islets, but the islets from reverted diabetics showed abundant insulin immunoreactivity (red: insulin, green: glucagon, blue: DAPI) Scale bar: 50 μ m.

3.2. Metabolic Panel from Blood and Urine in Diabetic Rats

The routinely used biochemical analysis of blood or urine from acute and chronic diabetic rats, insulin-treated diabetic rats, and reverted diabetic rats, as well as control rats, is summarized in Tables 4–7.

In diabetic rats, the carbamide content in urine increased significantly compared to the age-matched controls (acute: $p < 0.0001$; chronic: $p < 0.0001$). The levels of serum albumin of acute diabetics ($p < 0.01$) and total protein (TP) of chronic diabetics ($p < 0.01$) were lower than those of the age-matched control rats. The levels of the enzymes glutamic-pyruvic transaminase (GPT) and alkaline phosphatase (ALP) were both elevated, and in the case of ALP, the difference was significant when compared to controls ($p < 0.001$).

In the insulin-treated diabetic group, both the carbamide content in urine and the TP content in serum were at the control level despite diabetic alterations.

Urine pH was significantly lower in acute diabetic rats ($p < 0.05$), and even lower in the chronic diabetic group ($p < 0.05$), when compared to that of the age-matched controls. The urine test strip was positive for leukocytes in the chronic diabetics, and the positive result indicates the presence of 25 or more leukocytes per μ L.

In the insulin-treated diabetic group, urine pH value was similar to that of controls, and the test strip was positive for leukocytes.

Table 4. Metabolic panels from blood and urine of acute diabetic rats.

		Controls (n = 3)	Acute Diabetics (n = 4)
Carbamide (mmol/L)	Blood	9.31 \pm 0.97	9.61 \pm 0.81
	Urine	18.38 \pm 2.66	456.1 \pm 27.84 ****
Albumin (g/L)	Blood	34.0 \pm 0.0	31.0 \pm 0.41 **

Data are expressed as mean \pm SEM; ** $p < 0.01$; **** $p < 0.0001$ vs. controls.

Table 5. Metabolic panels from blood and urine of chronic diabetic rats.

		Controls (n = 5–20)	Chronic Diabetics (n = 3–14)	Insulin-Treated Diabetics (n = 4–13)	Reverted Diabetics (n = 3–4)
Carbamide (mmol/L)	Blood	9.37 ± 0.2	10.92 ± 0.42	8.0 ± 0.29 * ^{ooo}	9.63 ± 0.44
	Urine	27.43 ± 3.63	397.5 ± 26.56 ****	18.71 ± 2.99 ^{oooo}	-
Creatinine (µmol/L)	Blood	70.0 ± 6.4	83.88 ± 8.33	81.89 ± 5.47	88.25 ± 2.18
Albumin (g/L)	Blood	32.27 ± 0.88	29.55 ± 0.95	30.69 ± 1.15	34.0 ± 0.41
Cholesterol (mmol/L)	Blood	2.19 ± 0.05	2.35 ± 0.09	2.28 ± 0.09	3.26 ± 0.31 **
Triglyceride (mmol/L)	Blood	2.78 ± 1.26	1.94 ± 0.15	2.18 ± 0.2	2.27 ± 0.38
AST (U/L)	Blood	143.9 ± 10.47	132.0 ± 21.37	117.2 ± 8.99	117.8 ± 11.35
GPT (U/L)	Blood	68.22 ± 3.51	88.0 ± 7.5	61.44 ± 4.96	66.5 ± 6.4
ALP (U/L)	Blood	402.6 ± 26.63	1393 ± 184.9 ***	598.8 ± 91.04	423.5 ± 40.19
LDH (U/L)	Blood	603.4 ± 50.43	677.5 ± 30.17	616.0 ± 62.53	728.3 ± 46.25
Total protein (g/L)	Blood	65.04 ± 0.72	59.89 ± 1.11 **	59.54 ± 1.37 **	62.67 ± 1.21
Total bilirubin (mg/L)	Blood	6.11 ± 1.23	4.56 ± 1.06	3.15 ± 0.52	3.13 ± 1.08

Data are expressed as mean ± SEM; * $p < 0.05$; ** $p < 0.01$; *** $p < 0.001$; **** $p < 0.0001$ vs. controls; ^{ooo} $p < 0.001$; ^{oooo} $p < 0.0001$ vs. diabetics. (AST: aspartate aminotransferase, GPT: glutamic-pyruvic transaminase, ALP: alkaline phosphatase, LDH: lactate dehydrogenase).

Table 6. Metabolic panels from urine of acute diabetic rats.

	Controls (n = 3)	Acute Diabetics (n = 4)
Specific gravity	1.01 ± 0.0	1.01 ± 0.0
pH	7.33 ± 0.17	6.38 ± 0.24 *
Leukocytes	Negative	negative
Nitrite	Negative	negative
Ketones	Negative	negative

Data are expressed as mean ± SEM; * $p < 0.05$ vs. controls.

Table 7. Metabolic panels from urine of chronic diabetic rats.

	Controls (n = 5)	Chronic Diabetics (n = 3)	Insulin-Treated Diabetics (n = 4)
Specific gravity	1.0 ± 0.0	1.01 ± 0.0	1.0 ± 0.0
pH	7.1 ± 0.33	5.5 ± 0.0 *	7.0 ± 0.35 °
Leukocytes	negative	Positive	positive
Nitrite	negative	Negative	negative
Ketones	negative	Negative	negative

Data are expressed as mean ± SEM; * $p < 0.05$ vs. controls; ° $p < 0.05$ vs. diabetics.

3.3. Complete Blood Count in Acute and Chronic Diabetic Rats

The effect of hyperglycemia or insulin treatment on hematological parameters is summarized in Tables 8 and 9. The results showed that in the complete blood count, the only parameter that differed in acute diabetic rats from that in age-matched controls was the mean platelet volume (MPV), which was decreased ($p < 0.01$).

Table 8. Complete blood count including red blood cell, white blood cell, and platelet counts and blood cell indices of acute diabetic rats.

	Controls (n = 3)	Acute Diabetics (n = 4)
RBC, Red Blood Cell ($\times 10^6/\mu\text{L}$)	7.27 \pm 0.13	7.42 \pm 0.08
HCT, Hematocrit (%)	46.5 \pm 0.98	49.0 \pm 0.85
Hb, Hemoglobin (g/dL)	14.1 \pm 0.21	13.75 \pm 0.23
MCV, Mean corpuscular volume (fl)	64.03 \pm 2.26	66.03 \pm 0.84
MCH, mean corpuscular hemoglobin (pg)	19.4 \pm 0.59	18.5 \pm 0.2
MCHC, Mean corpuscular hemoglobin concentration (g/dL)	30.3 \pm 0.2	28.05 \pm 0.42
CHCM, Corpuscular hemoglobin concentration mean (g/dL)	30.2 \pm 0.23	27.9 \pm 0.47
CH, Corpuscular hemoglobin content (pg)	19.37 \pm 0.61	18.45 \pm 0.14
HDW, Hemoglobin concentration distribution width (g/dL)	2.2 \pm 0.05	1.99 \pm 0.09
RDW, Red blood cell volume distribution width (%)	11.53 \pm 0.35	11.33 \pm 0.31
WBC, White blood cell ($\times 10^3/\mu\text{L}$)	6.09 \pm 1.44	7.57 \pm 1.39
Lymphocyte count ($\times 10^3/\mu\text{L}$)	4.29 \pm 1.4	5.47 \pm 1.14
Monocyte count ($\times 10^3/\mu\text{L}$)	0.18 \pm 0.04	0.29 \pm 0.07
Neutrophil count ($\times 10^3/\mu\text{L}$)	1.2 \pm 0.05	1.2 \pm 0.1
Eosynophil count ($\times 10^3/\mu\text{L}$)	0.22 \pm 0.06	0.39 \pm 0.14
Basophil count ($\times 10^3/\mu\text{L}$)	0.04 \pm 0.003	0.05 \pm 0.005
Large unstained cell count ($\times 10^3/\mu\text{L}$)	0.16 \pm 0.06	0.17 \pm 0.04
PLT, Platelet count ($\times 10^3/\mu\text{L}$)	663.0 \pm 33	960.8 \pm 181.9
MPV, Mean platelet volume (fl)	9.03 \pm 2.13	7.85 \pm 0.19 **

Data are expressed as mean \pm SEM; ** $p < 0.01$ vs. controls.

The blood of chronic diabetic rats was thickened, and the RBC count ($p < 0.001$), the hematocrit ($p < 0.001$), and the Hb concentration ($p < 0.01$) was significantly increased compared to those of controls. Furthermore, the Hb concentration distribution width (HDW, $p < 0.001$) was decreased compared to that of controls.

In the insulin-treated diabetic and reverted diabetic animals, the measured hematological parameters were similar to the values of age-matched controls.

Table 9. Complete blood count including red blood cell, white blood cell, and platelet counts and blood cell indices of chronic diabetic rats.

	Controls (n = 13–18)	Chronic Diabetics (n = 12–13)	Insulin-Treated Diabetics (n = 6–12)	Reverted Diabetics (n = 3–4)
RBC, Red Blood Cell ($\times 10^6/\mu\text{L}$)	8.43 \pm 0.13	9.34 \pm 0.11 ***	8.59 \pm 0.18 °	8.77 \pm 0.18
HCT, Hematocrit (%)	46.94 \pm 0.75	52.42 \pm 0.56 ***	49.34 \pm 1.24	50.53 \pm 2.37
Hb, Hemoglobin (g/dL)	14.48 \pm 0.21	15.74 \pm 0.2 **	15.11 \pm 0.19	16.08 \pm 0.55
MCV, Mean corpuscular volume (fl)	55.68 \pm 0.53	56.13 \pm 0.45	57.54 \pm 0.63	57.6 \pm 1.96
MCH, Mean corpuscular hemoglobin (pg)	17.18 \pm 0.18	16.87 \pm 0.19	17.66 \pm 0.24	18.33 \pm 0.5
MCHC, Mean corpuscular hemoglobin concentration (g/dL)	30.88 \pm 0.35	30.03 \pm 0.24	30.74 \pm 0.59	31.85 \pm 0.5
CHCM, Corpuscular hemoglobin concentration mean (g/dL)	30.28 \pm 0.29	29.79 \pm 0.15	29.72 \pm 0.47	30.9 \pm 0.24
CH, Corpuscular hemoglobin content (pg)	16.79 \pm 0.15	16.69 \pm 0.1	17.02 \pm 0.22	17.78 \pm 0.65
HDW, Hemoglobin concentration distribution width (g/dL)	2.74 \pm 0.06	2.34 \pm 0.06 ***	2.58 \pm 0.06	2.85 \pm 0.16 °
RDW, Red blood cell volume distribution width (%)	13.72 \pm 0.35	12.17 \pm 0.22	13.03 \pm 0.3	14.35 \pm 1.16
WBC, White blood cell ($\times 10^3/\mu\text{L}$)	6.0 \pm 0.32	6.08 \pm 0.39	6.62 \pm 0.37	6.08 \pm 0.69
Lymphocyte count ($\times 10^3/\mu\text{L}$)	4.07 \pm 0.29	3.76 \pm 0.31	4.67 \pm 0.29	5.19 \pm 0.37
Monocyte count ($\times 10^3/\mu\text{L}$)	0.18 \pm 0.02	0.17 \pm 0.02	0.15 \pm 0.02	0.17 \pm 0.02
Neutrophil count ($\times 10^3/\mu\text{L}$)	1.37 \pm 0.09	1.69 \pm 0.17	1.32 \pm 0.12	1.33 \pm 0.26
Eosynophil count ($\times 10^3/\mu\text{L}$)	0.18 \pm 0.04	0.15 \pm 0.02	0.12 \pm 0.01	0.12 \pm 0.01
Basophil count ($\times 10^3/\mu\text{L}$)	0.03 \pm 0.003	0.04 \pm 0.005	0.04 \pm 0.006	0.04 \pm 0.005
Large unstained cell count ($\times 10^3/\mu\text{L}$)	0.2 \pm 0.04	0.2 \pm 0.06	0.18 \pm 0.06	0.14 \pm 0.02
PLT, Platelet count ($\times 10^3/\mu\text{L}$)	819 \pm 49.71	643.8 \pm 26.79	881.7 \pm 113.3	903 \pm 56.08
MPV, Mean platelet volume (fl)	7.81 \pm 0.17	6.93 \pm 0.2	7.9 \pm 0.41	8.95 \pm 0.21 °°
Reticulocyte count ($\times 10^3/\mu\text{L}$)	205.5 \pm 13.19	169.7 \pm 7.13	193.8 \pm 9.58	225.3 \pm 16.62
MCVr, Reticulocyte mean corpuscular volume (fl)	69.22 \pm 0.91	70.13 \pm 0.71	70.52 \pm 0.95	71.7 \pm 1.82
CHCMr, Reticulocyte hemoglobin concentration mean (g/dL)	27.2 \pm 0.15	27.28 \pm 0.2	26.88 \pm 0.18	27.65 \pm 0.16 #
CHr, Mean reticulocyte hemoglobin (pg)	18.8 \pm 0.2	19.05 \pm 0.3	18.86 \pm 0.26	19.75 \pm 0.55

Data are expressed as mean \pm SEM; ** $p < 0.01$; *** $p < 0.001$ vs. controls; ° $p < 0.05$; °° $p < 0.01$ vs. diabetics; # $p < 0.05$ vs. insulin-treated diabetics.

3.4. Diameter and Morphology of Red Blood Cells

The result of the complete blood count test justified the detailed investigation of oxidative-stress-related changes in RBCs. The diameter of RBCs was quantified from smears made from whole blood of chronic diabetic, insulin-treated diabetic, and control rats (Figures 2 and 3). In control rats, the average RBC diameter was $5.49 \pm 0.001 \mu\text{m}$, which resulted from a normal curve; the diameter was 5 to $6 \mu\text{m}$ in 63.5% of RBCs, and ranged from 4 to $5 \mu\text{m}$ and 6 to $7 \mu\text{m}$ in 17.9% of RBCs.

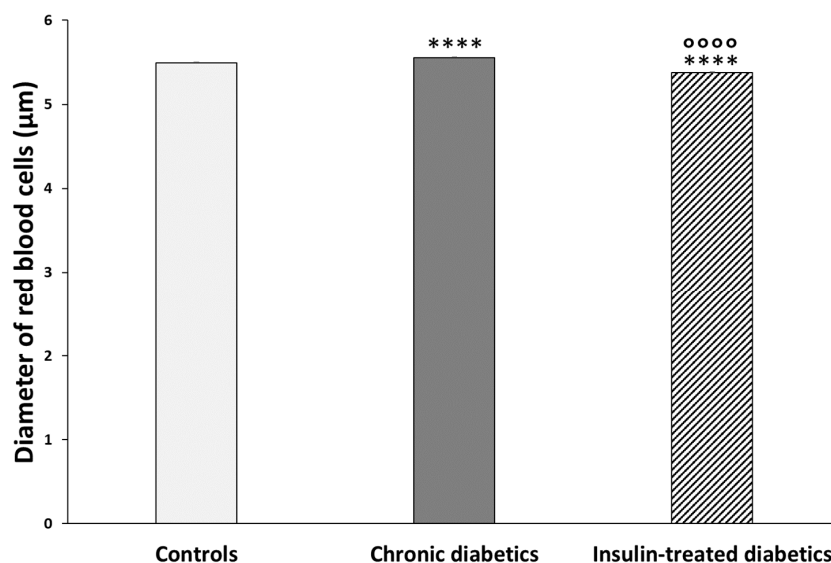


Figure 2. The diameter of red blood cells in control, chronic diabetic, and insulin-treated diabetic rats. The diameter of red blood cells increased in chronic diabetic groups, and decreased in the insulin-treated diabetic group. Data are expressed as mean \pm SEM; **** $p < 0.0001$ vs. controls; ○○○○ $p < 0.0001$ vs. diabetics.

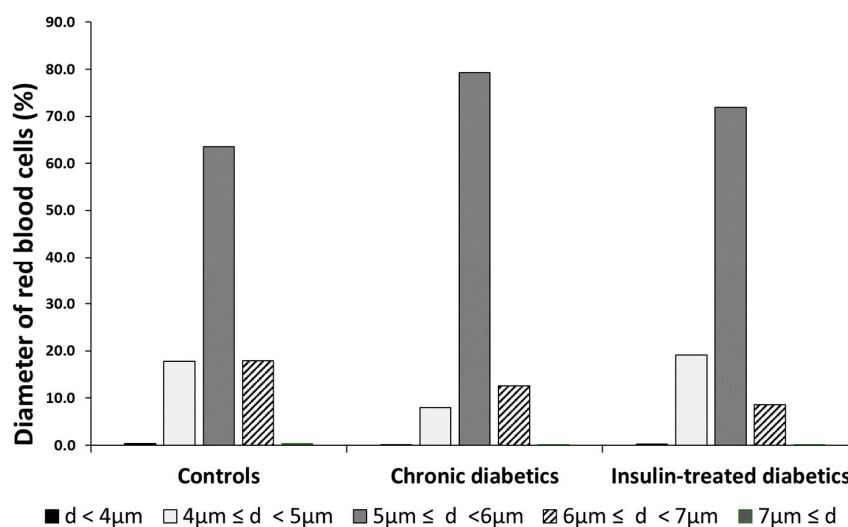


Figure 3. Diameter distribution of red blood cells in control, chronic diabetic, and insulin-treated diabetic rats. Decrease in the diameter distribution width was seen in the chronic diabetic and insulin-treated diabetic groups, and it was more pronounced in the chronic diabetic group.

The average RBC diameter of chronic diabetics was significantly higher ($5.55 \pm 0.01 \mu\text{m}$, $p < 0.0001$) compared to that of the controls.

In insulin-treated diabetics, the average RBC diameter decreased ($5.38 \pm 0.01 \mu\text{m}$, $p < 0.0001$) compared to that of the controls, and this change (represented in Figure 3) resulted from an increase in the percentage of the 4 to 5 μm ranges (19.1%) and a decrease in the percentage of the 6 to 7 μm range (8.6%).

The morphology of RBCs was examined on pictures from blood smears made at $1000\times$ magnification (Figure 4). Table 10 summarizes the morphological changes of RBCs in the chronic diabetic, insulin-treated diabetic, and the age-matched control groups. In the chronic diabetics, the eccentrocyte (Table 10, Figure 5a; $p < 0.001$), hemolyzed RBC (Table 10, Figure 5b; $p < 0.001$), and codocyte (Table 10, Figure 5c; $p < 0.0001$) shapes occurred

more often compared to the controls. In the insulin-treated diabetics, the frequency of eccentrocytes and hemolyzed RBCs was similar to that of controls, and the percentage of codocytes was significantly lower compared to that of diabetics ($p < 0.05$); however it was higher compared to that of controls ($p < 0.0001$). Other shape abnormalities, such as those of acanthocyte, ovalocyte, dacrocyte, and schistocyte, also occurred in greater proportion in the insulin-treated diabetic group compared to the controls and/or diabetics.

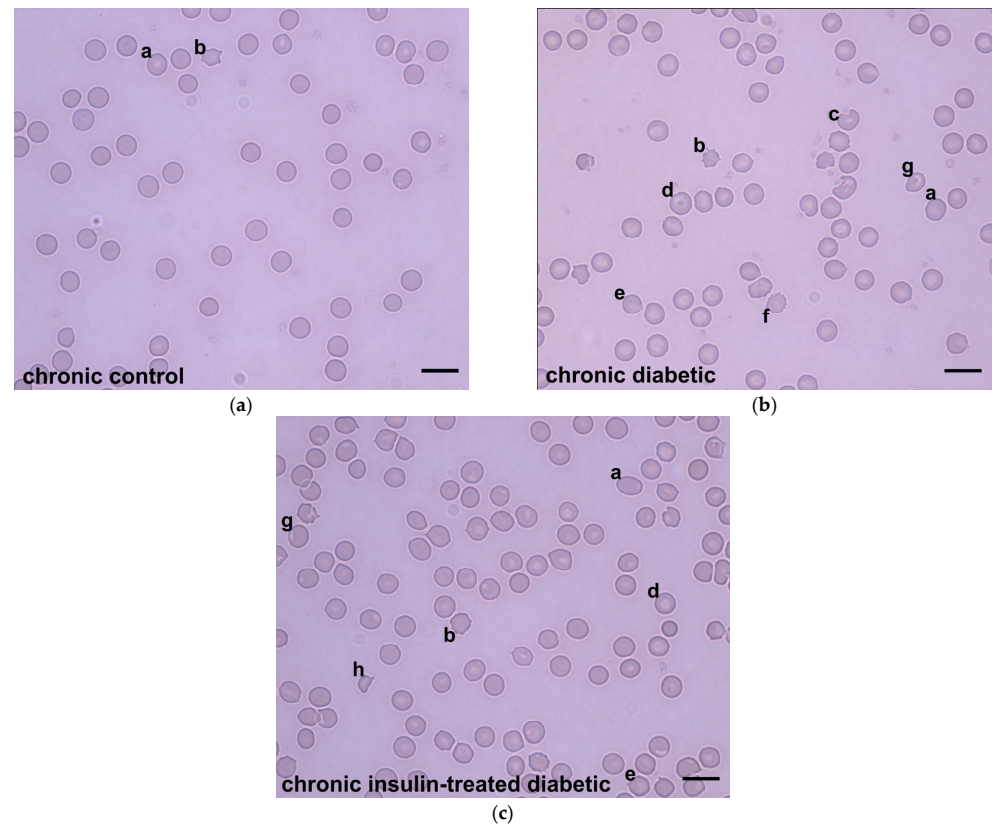


Figure 4. Representative micrograph of blood smears from (a) control, (b) chronic diabetic, and (c) insulin-treated diabetic rats. Scale bar 10 μ m. a: ovalocyte, b: acanthocyte, c: hemolyzed red blood cell, d: codocyte, e: dacrocyte, f: echinocyte, g: eccentrocyte, h: schistocyte.

Table 10. Morphological changes of red blood cells in chronic diabetic rats.

	Controls	Chronic Diabetics	Insulin-Treated Diabetics
Echinocyte (Burr cells; %)	2.87 \pm 0.5	3.39 \pm 0.45	3.01 \pm 0.44
Acanthocyte (Spur cells; %)	1.24 \pm 0.41	0.59 \pm 0.16	2.67 \pm 0.48 ^{**\circ}
Ovalocyte (%)	11.7 \pm 1.27	7.51 \pm 0.69	15.63 \pm 1.48 ^{$\circ$$\circ$$\circ$$\circ$}
Dacrocyte (Teardrop cells; %)	1.48 \pm 0.32	2.48 \pm 0.38	4.32 \pm 0.7 ^{***}
Schistocyte (Fragmented cells; %)	0.67 \pm 0.18	0.89 \pm 0.19	1.73 \pm 0.26 ^{**}
Eccentrocyte (%)	0.0 \pm 0.0	0.61 \pm 0.2 ^{***}	0.06 \pm 0.03 ^{\circ}
Hemolyzed RBC (%)	0.32 \pm 0.11	1.48 \pm 0.3 ^{***}	0.5 \pm 0.12 ^{\circ}
Codocyte (Target cells; %)	0.0 \pm 0.0	8.17 \pm 1.21 ^{****}	2.48 \pm 0.36 ^{****\circ}

Data are expressed as mean \pm SEM; ^{**} $p < 0.01$; ^{***} $p < 0.001$; ^{****} $p < 0.0001$ vs. controls; ^{\circ} $p < 0.05$; ^{\circ \circ} $p < 0.01$; ^{\circ \circ \circ \circ} $p < 0.0001$ vs. diabetics. (RBC: red blood cell).

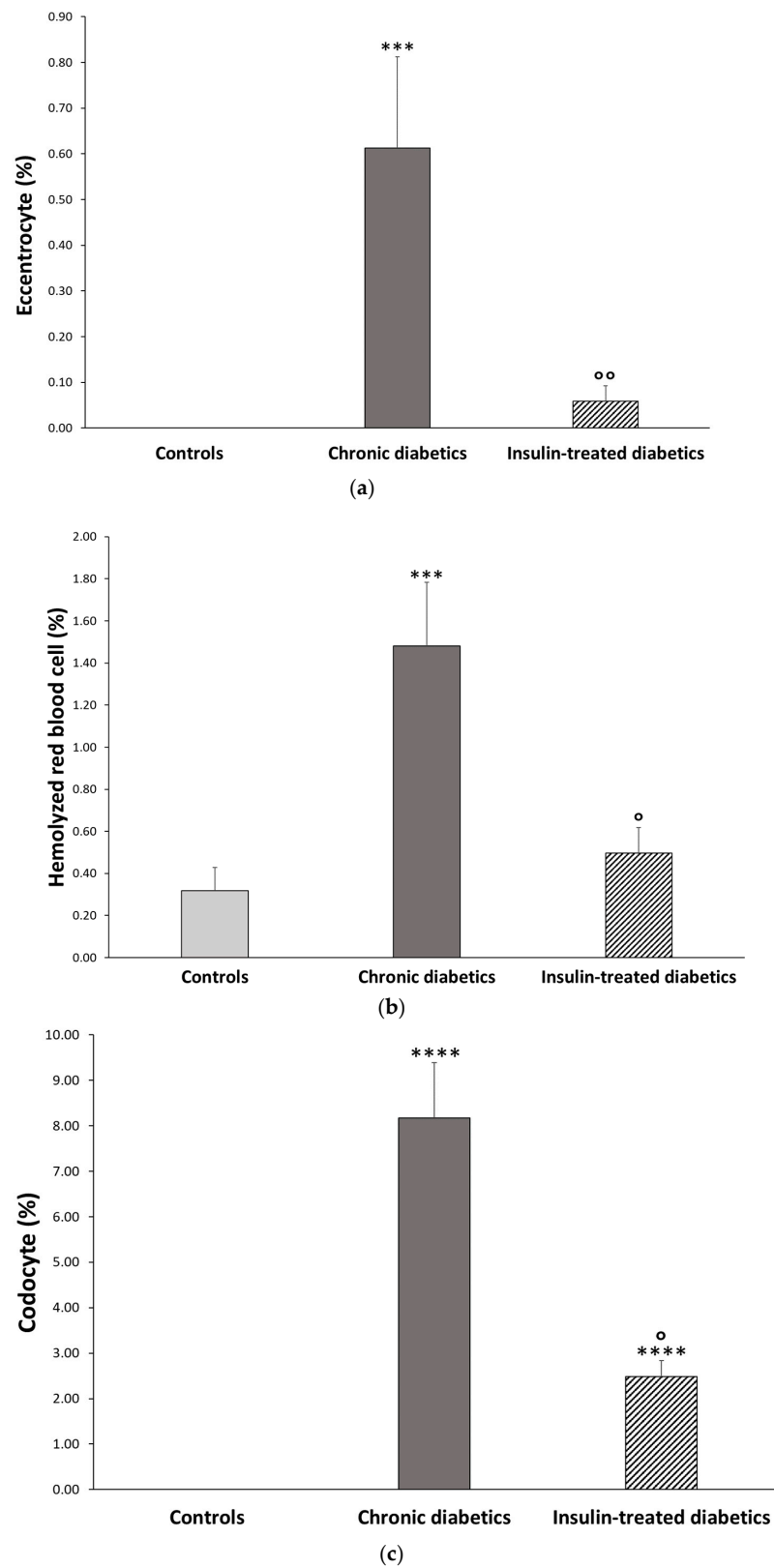
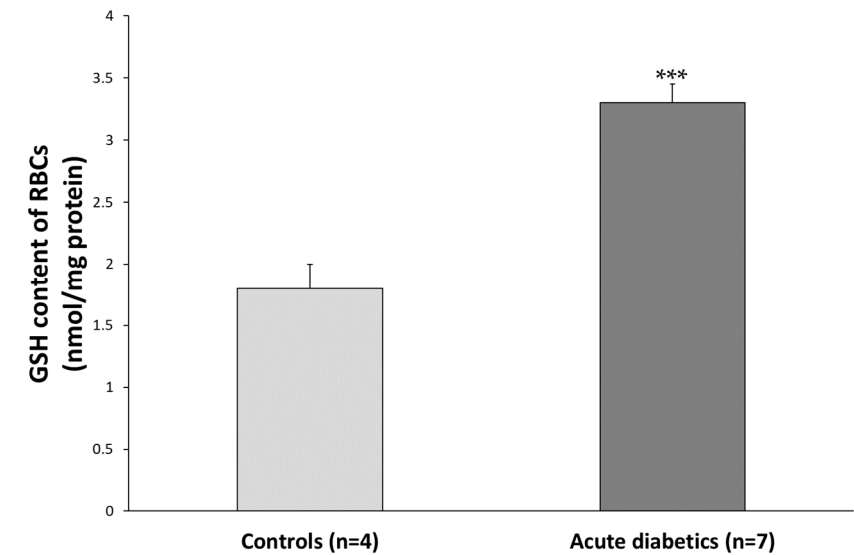


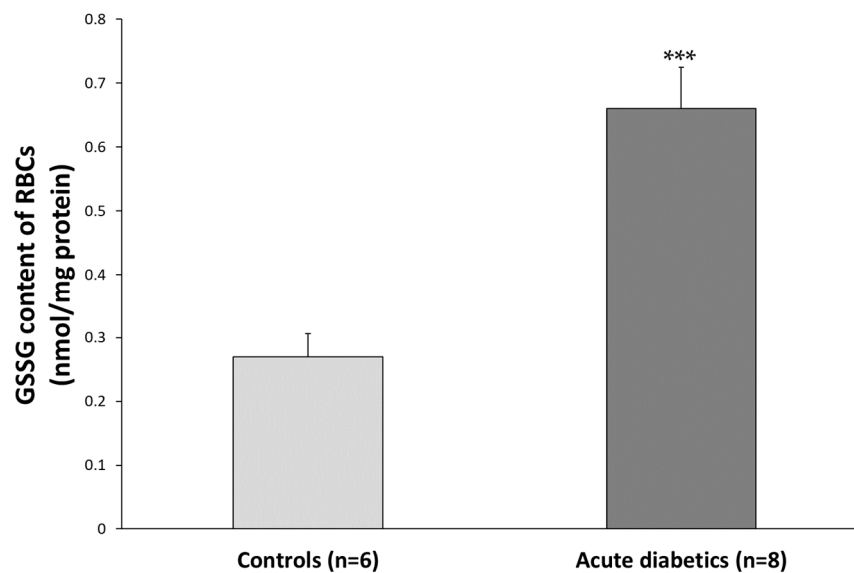
Figure 5. Morphology of red blood cells in smears from controls, chronic diabetics, and insulin-treated diabetics. The (a) eccentrocyte, (b) hemolyzed red blood cell, and (c) codocyte shapes occurred more frequently in the smears of chronic diabetic rats compared to those of the controls; moreover, a lower proportion was found in the insulin-treated diabetic rats compared to the diabetics. Data are expressed as mean \pm SEM; *** $p < 0.001$, **** $p < 0.0001$ vs. controls; ° $p < 0.05$, °° $p < 0.01$ vs. diabetics.

3.5. The Reduced and Oxidized Glutathione Content of Red Blood Cells

The antioxidant peptide GSH and its oxidized form were measured in RBCs of acute diabetics and their controls (Figure 6), as well as chronic diabetic, insulin-treated diabetic, and their control rats (Figure 7). Furthermore, the ratio of GSH to GSSG was calculated as an indicator of altered redox potential in the system (Figures S1 and S2).



(a)



(b)

Figure 6. (a) Reduced form of glutathione (GSH) and (b) oxidized form of glutathione (GSSG) content of RBCs in acute diabetic and control rats. In acute diabetics, both the GSH and GSSG content were almost doubled compared to that of the controls. Data are expressed as mean \pm SEM; *** $p < 0.001$ vs. controls.

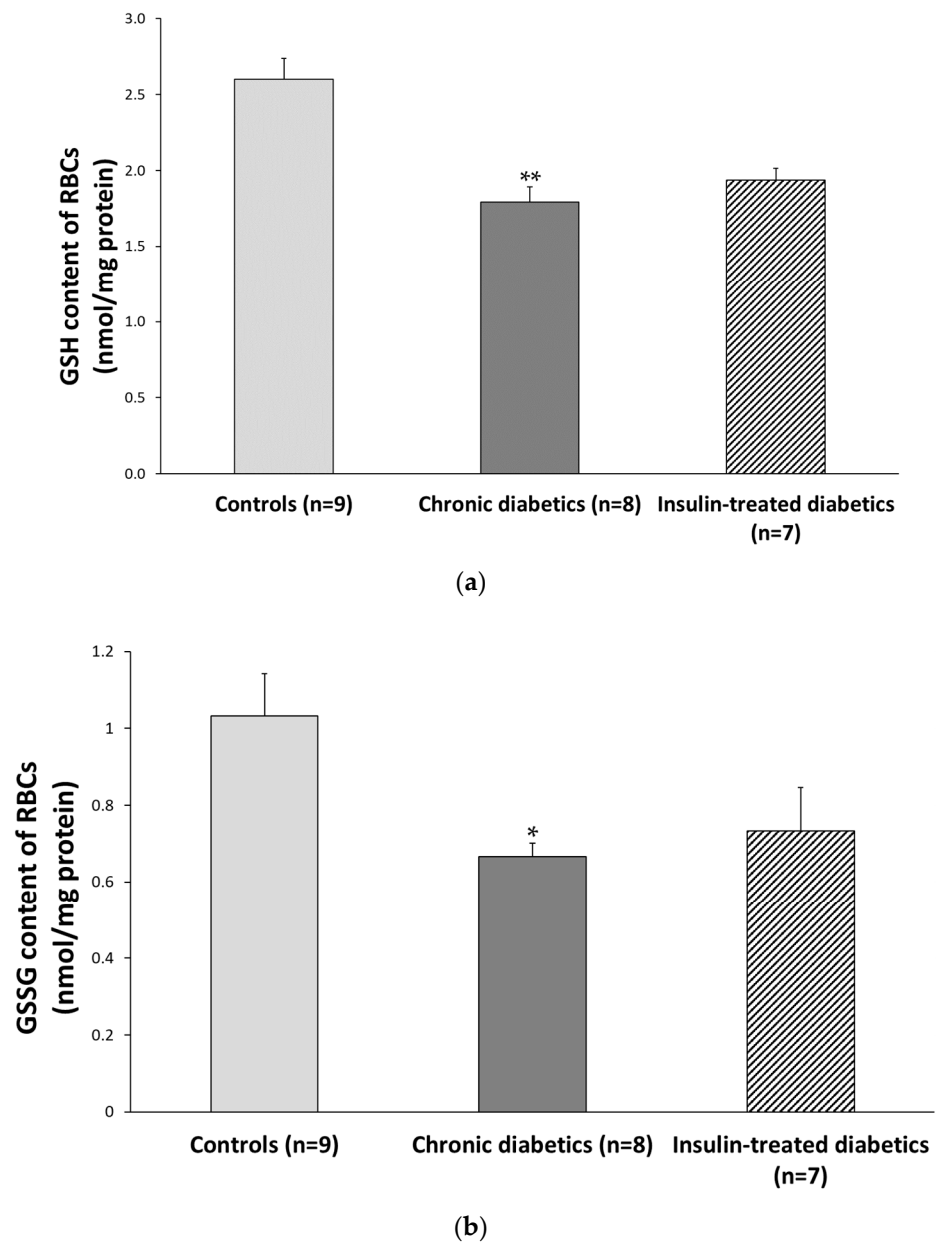


Figure 7. (a) Reduced form of glutathione (GSH) and (b) oxidized form of glutathione (GSSG) content of RBCs in chronic diabetic, insulin-treated diabetic, and age-matched control rats. Both the reduced and the oxidized form of glutathione decreased markedly in RBCs of chronic diabetic and insulin-treated diabetic rats compared to those of the controls. Data are expressed as mean \pm SEM; * $p < 0.05$, ** $p < 0.01$ vs. controls.

In the RBC populations of acute diabetics, both the GSH and GSSG levels were almost doubled compared to those of the controls (GSH: 3.3 ± 0.15 nmol/mg protein vs. 1.8 ± 0.2 nmol/mg protein, $p < 0.001$; GSSG: 0.66 ± 0.07 nmol/mg protein vs. 0.27 ± 0.04 nmol/mg protein, $p < 0.001$).

In contrast, 10 weeks after STZ injection, GSH and GSSG levels were lower in both diabetic and insulin-treated diabetic rats when compared to those of the controls. The decrease was about 30% in the case of GSH (diabetics: 1.79 ± 0.1 nmol/mg protein; insulin-treated diabetics: 1.94 ± 0.08 nmol/mg protein vs. 2.6 ± 0.14 nmol/mg protein, $p < 0.01$) and around 35–40% for GSSG (diabetics: 0.67 ± 0.03 nmol/mg protein; insulin-treated diabetics: 0.73 ± 0.11 nmol/mg protein vs. 1.03 ± 0.11 nmol/mg protein, $p < 0.05$).

No significant change in the ratio of the reduced and oxidized form was observed during any of the treatments (acute: 5.7 ± 0.41 vs. 7.07 ± 0.81 ; chronic diabetics: 2.66 ± 0.14 ; insulin-treated diabetics: 2.37 ± 0.07 vs. 2.35 ± 0.07).

4. Discussion

The aim of the present study was to investigate the alterations caused by oxidative stress in routinely used clinical parameters measured from blood and urine, and on the morphology of RBCs, in a widely used STZ-diabetic rat model. These alterations may contribute to the pathophysiology of diabetes mellitus and its complications, such as microvascular disturbances.

A single dose of STZ led to body weight loss, extremely high levels of blood and urine glucose, and elevated HbA1c value and percentage. Interestingly, in some cases, diabetic rats became spontaneously normoglycemic and their blood glucose level decreased below 18 mmol/L during the ten-week experimental period; these rats were grouped as reverted diabetics. The representative double-labeled fluorescent micrographs against insulin and glucagon showed the lack of insulin-producing pancreatic beta cells in diabetics and insulin-treated diabetics. In the case of reverted diabetics, we detected insulin-positive cells in Langerhans islets surrounded by a major mass of glucagon-immunoreactive cells. Further studies are required to elucidate the underlying mechanisms. In the past decade, some effort has been dedicated to replace the lost beta cells in the therapy of diabetes mellitus. Recently, researchers found that alpha cells, as a replacement for beta cells, may be a potential target for the production of insulin. One of the most important reasons for this new therapeutic strategy is the ability of alpha cells to be spontaneously converted into insulin-producing cells [22–24].

The routinely used metabolic panel measurements from blood or urine showed the most remarkable changes in diabetic groups. The urine carbamide level was increased in acute as well as in chronic diabetics; however, blood carbamide levels were similar to those of the control. These blood results indicate normal renal function [25], and the urine results highlight increased protein catabolism consistent with the reduced weight gain of diabetic rats and the elevated blood ALP level of chronic diabetics [26,27]. Elevated serum GPT and ALP levels, and decreased serum albumin and TP levels, of diabetics are in line with earlier studies [28,29]. These results raise the possibility of liver damage because ALP and GPT levels in the blood are the most important indicators of hepatic injury [28]. On the other hand, low albumin and TP levels not only reflect hepatic failure, but also oxidative status, since they are antioxidant marker proteins. Moreover, albumin is the most abundant extracellular protein and plays an important role in buffering serum redox status [30]. The effects of insulin on metabolic parameters were revealed in insulin-treated diabetic and reverted diabetic groups. Both spontaneously recovered, and endogenously and exogenously administered insulins were effective, with the measured parameters being similar to those of controls, except for the TP level. These results are consistent with the findings of Mohamed A. et al. [31], where the effectiveness of insulin in inhibiting hepatic injury was shown using biochemical and histological parameter monitoring.

The routinely used complete blood count revealed changes only in the chronic diabetic group when compared to controls. We measured increased levels in RBC indices, namely RBC count, hematocrit, and Hb concentration, but a decreased level of HDW. Our observations correlate with the findings of others [5,32]. These findings could result from the extremely high glucose concentration causing blood thickening, or the lack of insulin. Moreover, insulin may stimulate the proliferation of erythroid progenitor cells [33]. The complete blood count of insulin-treated diabetics and reverted diabetics was similar to that of control data.

The complete blood count test showed alteration in RBC count and in RBC-derived parameters. Therefore, our further investigations focused on the morphological changes and altered oxidative status of RBCs, since RBCs play an important role in microcirculation and they are vulnerable to a hyperglycemic environment. We found that the diameter

of RBCs increased and abnormally shaped RBCs occurred more often in diabetics compared to controls, in line with other studies [11,34]. We observed eccentrocytes, hemolyzed RBCs, and codocytes in larger proportions in diabetic smears. The flexibility of RBCs is very important for their free passage through capillaries, transporting oxygen or carbon monoxide, and this property is highly influenced by the cell shape [35]. On the other hand, these abnormal shapes, namely, those of eccentrocytes, hemolyzed RBCs, and codocytes, may be caused by oxidative stress [19,36,37]. An eccentrocyte is a special form of RBC in which Hb is shifted to one side of the cell because of the oxidative damage to the cell membrane and cytoskeleton [38]. Increased hemolysis was described in the pathomechanism of some oxidative-stress-related diseases, such as diabetes mellitus, sepsis, or sickle cell disease [19,39–41]. Codocytes also occur in diseases accompanied by oxidative stress, such as diabetes mellitus, beta-thalassemia, or autism spectrum disorders [11,36,42]. In insulin-treated diabetics, we observed that the occurrence of eccentrocytes and hemolyzed RBCs was similar to that of controls. However, codocytes were present in insulin-treated groups, and their frequency was one-third of that observed in the diabetic samples. The highest occurrence of other RBC morphologies, namely acanthocytes, ovalocytes, dacrocytes, and schistocytes, was found in smears of insulin-treated diabetic rats compared to the controls and/or diabetics. This result is in line with earlier findings that exogenously administered insulin may be ineffective in some aspects of diabetes-related alterations [43–45]. Insulin is a drug that can induce immune-mediated hemolysis, which may explain the increased proportion of schistocytes in insulin-treated diabetic rats [46].

The complete blood count test suggests platelet abnormalities in both acute and chronic diabetic rats, in addition to reverted diabetic rats. However, prothrombotic events are seen frequently in diabetic patients [47]. Earlier findings about paradoxical results of *in vivo* and *in vitro* studies highlight possible compensatory mechanisms in long-lasting diabetes [48].

To gain insights into the antioxidant status of RBCs, we determined the GSH and GSSG level and the ratio of GSH to GSSG in RBC populations. Furthermore, summarizing the data from acute and chronic studies, we obtained a time–response curve of the antioxidant capacity of diabetic RBCs. The doubled value of both the GSH and GSSG is not only a sign of a prompt antioxidant response to STZ injection, but also indicates a balanced free radical/oxidant pool. In contrast, 10 weeks after STZ injection, the decreased levels of GSH and GSSG may indicate some kind of adaptation to the system, along with the exhaustion of the defense response. This reduction in GSH and GSSG levels in the chronic experiment is in agreement with other studies [49,50]. Dincer et al. [50] investigated the GSH pathway involving the GSH level, GSHPx, and GR in RBCs of well-controlled and poorly controlled type 1 diabetic patients versus healthy subjects at the baseline and after 2 h of incubation with H₂O₂. The greatest decrease for all investigated components was in poorly controlled diabetic patients at baseline. The 2 h incubation of RBCs with H₂O₂ impaired the GSH pathway in all groups, and it was most pronounced in the poorly controlled diabetic group. However, in our system, the fact that the ratio of oxidized and reduced glutathione did not change significantly in acute and chronic samples may indicate that the activities of the crucial enzymes such as GSHPx and GR were unchanged.

There are several limitations to our study. However, considering the complexity of diabetic metabolic alterations, further investigations are needed to examine correlations and gain comprehensive results. The hyperglycemia associated with the altered oxidant/antioxidant status in diabetic and reverted diabetic RBCs will be of interest.

5. Conclusions

In conclusion, long-lasting hyperglycemia altered RBC indices—namely, RBC count, hematocrit, hemoglobin concentration, and hemoglobin concentration distribution width—and the diameter of RBCs. Abnormal RBC shapes, such as those of the eccentrocyte, hemolyzed RBC, and codocyte, occurred more often in the chronic diabetic group. The GSH content of RBCs showed time-dependent changes. This indicates that, after an initial increase, the level of GSH decreased; therefore, this defense system may be exhausted in

a long-lasting pro-oxidant environment. Our results suggest the damage to RBCs may contribute to the microvascular complications in diabetes mellitus. The effectiveness of insulin treatment for several investigated parameters emphasizes the importance of a well-adjusted insulin treatment for diabetic patients.

Supplementary Materials: The following supporting information can be downloaded at: <https://www.mdpi.com/article/10.3390/app13179920/s1>, Figure S1: The ratio of reduced/oxidized glutathione (GSH/GSSG) in the RBC population of acute diabetic and control rats; Figure S2: The ratio of reduced/oxidized glutathione (GSH/GSSG) in the RBC population of chronic diabetic, insulin-treated diabetic, and control rats.

Author Contributions: Conceptualization, M.B., N.B. and E.H.; methodology, M.B. and N.B.; validation, N.B.; investigation, A.M.B., Á.F. and Z.S.; resources, Z.S.; writing—original draft preparation, Z.S.; writing—review and editing, M.B., N.B. and E.H.; visualization, M.B.; supervision, N.B.; funding acquisition, N.B. All authors have read and agreed to the published version of the manuscript.

Funding: This research was funded by the Hungarian NKFIH fund project, No. FK131789 (N.B.); János Bolyai Research Scholarship of the Hungarian Academy of Sciences (N.B.) and ÚNKP-22-5—New National Excellence Program of the Ministry for Innovation and Technology from the source of the National Research, Development and Innovation Fund (N.B.).

Institutional Review Board Statement: In all procedures involving experimental animals, the principles of the National Institutes of Health (Bethesda, MD, USA) guidelines and the EU directive 2010/63/EU for the protection of animals used for scientific purposes were strictly followed, and all the experiments were approved by the National Scientific Ethical Committee on Animal Int. J. Mol. Sci. 2023, 24, x FOR PEER REVIEW 14 of Experimentation (National Competent Authority), with the license number XX./1636/2019 and Animal Welfare Committee University of Szeged with the license number I-74-11/2019 MÁB.

Informed Consent Statement: Not applicable.

Data Availability Statement: Dataset available from the corresponding author at bmarsci@bio.u-szeged.hu e-mail address.

Conflicts of Interest: The authors declare no conflict of interest.

References

1. Sarwar, N.; Gao, P.; Seshasai, S.R.; Gobin, R.; Kaptoge, S.; Di Angelantonio, E.; Ingelsson, E.; Lawlor, D.A.; Selvin, E.; Stampfer, M.; et al. Diabetes mellitus, fasting blood glucose concentration, and risk of vascular disease: A collaborative meta-analysis of 102 prospective studies. *Lancet* **2010**, *375*, 2215–2222. [[CrossRef](#)] [[PubMed](#)]
2. Beckman, J.A.; Creager, M.A. Vascular Complications of Diabetes. *Circ. Res.* **2016**, *118*, 1771–1785. [[CrossRef](#)] [[PubMed](#)]
3. Zhou, Z.; Mahdi, A.; Tratsiakovich, Y.; Zahorán, S.; Kövamees, O.; Nordin, F.; Uribe Gonzalez, A.E.; Alvarsson, M.; Östenson, C.-G.; Andersson, D.C.; et al. Erythrocytes from Patients with Type 2 Diabetes Induce Endothelial Dysfunction Via Arginase I. *J. Am. Coll. Cardiol.* **2018**, *72*, 769–780. [[CrossRef](#)] [[PubMed](#)]
4. Palomino-Schätzlein, M.; Lamas-Domingo, R.; Ciudin, A.; Gutiérrez-Carcedo, P.; Marés, R.; Aparicio-Gómez, C.; Hernández, C.; Simó, R.; Herance, J.R. A Translational In Vivo and In Vitro Metabolomic Study Reveals Altered Metabolic Pathways in Red Blood Cells of Type 2 Diabetes. *J. Clin. Med.* **2020**, *9*, 1619. [[CrossRef](#)]
5. Alamri, B.; Bahabri, A.; Alderehim, A.A.; Alabduljabbar, M.; Alsubaie, M.M.; Alnaqeb, D.; Almogbel, E.; Metias, N.S.; Alotaibi, O.; Al-Rubeaan, K. Hyperglycemia effect on red blood cells indices. *Eur. Rev. Med. Pharmacol. Sci.* **2019**, *23*, 2139–2150.
6. Viskupicova, J.; Blaskovic, D.; Galiniak, S.; Soszyński, M.; Bartosz, G.; Horakova, L.; Sadowska-Bartos, I. Effect of high glucose concentrations on human erythrocytes in vitro. *Redox Biol.* **2015**, *5*, 381–387. [[CrossRef](#)]
7. Wang, Y.; Yang, P.; Yan, Z.; Liu, Z.; Ma, Q.; Zhang, Z.; Wang, Y.; Su, Y. The Relationship between Erythrocytes and Diabetes Mellitus. *J. Diabetes Res.* **2021**, *2021*, 6656062. [[CrossRef](#)]
8. Rajab, A.M.; Rahman, S.; Rajab, T.M.; Haider, K.H. Morphology and Chromic Status of Red Blood Cells Are Significantly Influenced by Gestational Diabetes. *J. Hematol.* **2018**, *7*, 140–148. [[CrossRef](#)]
9. Turpin, C.; Catan, A.; Guerin-Dubourg, A.; Debussche, X.; Bravo, S.B.; Álvarez, E.; Van Den Elsen, J.; Meilhac, O.; Rondeau, P.; Bourdon, E. Enhanced oxidative stress and damage in glycated erythrocytes. *PLoS ONE* **2020**, *15*, e0235335. [[CrossRef](#)]
10. Saleh, J. Glycated hemoglobin and its spinoffs: Cardiovascular disease markers or risk factors? *World J. Cardiol.* **2015**, *7*, 449–453. [[CrossRef](#)]

11. Neamțu, M.C.; Crăițoiu, S.; Avramescu, E.T.; Margină, D.M.; Băcănoiu, M.V.; Turneanu, D.; Danciulescu Miulescu, R. The prevalence of the red cell morphology changes in patients with type 2 diabetes mellitus. *Rom. J. Morphol. Embryol.* **2015**, *56*, 183–189. [[PubMed](#)]
12. Taneja, A.; Jagtap, M.; Shukla, S.; Vagha, S. Red Blood Cell Morphology in Diabetic Patients: A Case-control Study. *J. Clin. Diagn. Res.* **2022**, *16*, EC01–EC04. [[CrossRef](#)]
13. Xiong, Y.; Uys, J.D.; Tew, K.D.; Townsend, D.M. S-glutathionylation: From molecular mechanisms to health outcomes. *Antioxid. Redox. Signal.* **2011**, *15*, 233–270. [[CrossRef](#)] [[PubMed](#)]
14. Burak Çimen, M.Y. Free radical metabolism in human erythrocytes. *Clin. Chim. Acta* **2008**, *390*, 1–11. [[CrossRef](#)]
15. Izbéki, F.; Wittman, T.; Rosztóczy, A.; Linke, N.; Bódi, N.; Fekete, E.; Bagyánszki, M. Immediate insulin treatment prevents gut motility alterations and loss of nitrergic neurons in the ileum and colon of rats with streptozotocin-induced diabetes. *Diabetes Res. Clin. Pract.* **2008**, *80*, 192–198. [[CrossRef](#)]
16. Bódi, N.; Talapka, P.; Poles, M.Z.; Hermes, E.; Jancsó, Z.; Katarova, Z.; Izbéki, F.; Wittmann, T.; Fekete, E.; Bagyánszki, M. Gut Region-Specific Diabetic Damage to the Capillary Endothelium Adjacent to the Myenteric Plexus. *Microcirculation* **2012**, *19*, 316–326. [[CrossRef](#)]
17. Ford, J. Red blood cell morphology. *Int. J. Lab. Hematol.* **2013**, *35*, 351–357. [[CrossRef](#)]
18. KT, N.; Prasad, K.; Singh, B.M.K. Analysis of red blood cells from peripheral blood smear images for anemia detection: A methodological review. *Med. Biol. Eng. Comput.* **2022**, *60*, 2445–2462. [[CrossRef](#)]
19. Caldin, M.; Carli, E.; Furlanello, T.; Solano-Gallego, L.; Tasca, S.; Patron, C.; Lubas, G. A retrospective study of 60 cases of eccentrocytosis in the dog. *Vet. Clin. Pathol.* **2005**, *34*, 224–231. [[CrossRef](#)]
20. Lowry, O.H.; Rosebrough, N.J.; Farr, A.L.; Randall, R.J. Protein measurement with the Folin phenol reagent. *J. Biol. Chem.* **1951**, *193*, 265–275. [[CrossRef](#)]
21. Sedlak, J.; Lindsay, R.H. Estimation of total, protein-bound, and nonprotein sulfhydryl groups in tissue with Ellman's reagent. *Anal. Biochem.* **1968**, *25*, 192–205. [[CrossRef](#)] [[PubMed](#)]
22. Thorel, F.; Népote, V.; Avril, I.; Kohno, K.; Desgraz, R.; Chera, S.; Herrera, P.L. Conversion of adult pancreatic α -cells to β -cells after extreme β -cell loss. *Nature* **2010**, *464*, 1149–1154. [[CrossRef](#)] [[PubMed](#)]
23. Saleh, M.; Gittes, G.K.; Prasad, K. Alpha-to-beta cell trans-differentiation for treatment of diabetes. *Biochem. Soc. Trans.* **2021**, *49*, 2539–2548. [[CrossRef](#)] [[PubMed](#)]
24. Lu, J.; Jaafer, R.; Bonnavion, R.; Bertolino, P.; Zhang, C.X. Transdifferentiation of pancreatic α -cells into insulin-secreting cells: From experimental models to underlying mechanisms. *World J. Diabetes* **2014**, *5*, 847–853. [[CrossRef](#)] [[PubMed](#)]
25. Bamanikar, S.; Bamanikar, A.; Arora, A. Study of Serum urea and Creatinine in Diabetic and non-diabetic patients in a tertiary teaching hospital. *J. Med. Res.* **2016**, *2*, 12–15. [[CrossRef](#)]
26. Møller, N.; Nair, K.S. Diabetes and Protein Metabolism. *Diabetes* **2008**, *57*, 3–4. [[CrossRef](#)]
27. Abu-Lebdeh, H.S.; Nair, K.S. Protein metabolism in diabetes mellitus. *Baillieres Clin. Endocrinol. Metab.* **1996**, *10*, 589–601. [[CrossRef](#)]
28. Mohamed, J.; Nazratun Nafizah, A.H.; Zariyantey, A.H.; Budin, S.B. Mechanisms of Diabetes-Induced Liver Damage: The role of oxidative stress and inflammation. *Sultan Qaboos Univ. Med. J.* **2016**, *16*, e132–e141. [[CrossRef](#)]
29. Hasan, H.R.; Abdulsattar, A. Influence of diabetes disease on concentration of total protein, albumin and globulins in saliva and serum: A comparative study. *Iraqi Natl. J. Chem.* **2015**, *15*, 1–11.
30. Adnan Khalaf, M.; Ghassan Zainal, I. Investigation of Antioxidant Markers in Diabetic Patients. *Arch. Razi Inst.* **2021**, *76*, 1453–1460. [[CrossRef](#)]
31. Haidara, M.A.; Dallak, M.; El Karib, A.O.; Ellatif, M.A.; Eid, R.A.; Heidar, E.H.A.; Al-Ani, B. Insulin protects against hepatocyte ultrastructural damage induced by type 1 diabetes mellitus in rats. *Ultrastruct. Pathol.* **2018**, *42*, 508–515. [[CrossRef](#)] [[PubMed](#)]
32. Konsue, A.; Picheansoonthon, C.; Talubmook, C. Fasting Blood Glucose Levels and Hematological Values in Normal and Streptozotocin-Induced Diabetic Rats of *Mimosa pudica* L. Extracts. *Pharmacogn. J.* **2017**, *9*, 315–322. [[CrossRef](#)]
33. Miyagawa, S.-I.; Kobayashi, M.; Konishi, N.; Sato, T.; Ueda, K. Insulin and insulin-like growth factor I support the proliferation of erythroid progenitor cells in bone marrow through the sharing of receptors. *Br. J. Haematol.* **2000**, *109*, 555–562. [[CrossRef](#)] [[PubMed](#)]
34. Mohamed, J.; Shing, S.W.; Idris, M.H.M.; Budin, S.B.; Zainalabidin, S. The protective effect of aqueous extracts of roselle (*Hibiscus sabdariffa* L. UKMR-2) against red blood cell membrane oxidative stress in rats with streptozotocin-induced diabetes. *Clinics* **2013**, *68*, 1358–1363. [[CrossRef](#)]
35. Engström, K.G.; Ohlsson, L. Morphology and Filterability of Red Blood Cells in Neonatal and Adult Rats. *Pediatr. Res.* **1990**, *27*, 220–226. [[CrossRef](#)]
36. Bolotta, A.; Battistelli, M.; Falcieri, E.; Ghezzi, A.; Manara, M.C.; Manfredini, S.; Marini, M.; Posar, A.; Visconti, P.; Abruzzo, P.M. Oxidative Stress in Autistic Children Alters Erythrocyte Shape in the Absence of Quantitative Protein Alterations and of Loss of Membrane Phospholipid Asymmetry. *Oxidative Med. Cell. Longev.* **2018**, *2018*, 6430601. [[CrossRef](#)]
37. Senchenkova, E.Y.; Skvertchinskaya, E.; Dobrylko, I.; Sudnitsyna, J.; Gambaryan, S.; Mindukshev, I.; Gavins, F. Experimental oxidative stress-induced death of erythrocytes. *FASEB J.* **2017**, *31*, lb761.
38. Chan, T.K.; Chan, W.C.; Weed, R.I. Erythrocyte hemighosts: A hallmark of severe oxidative injury in vivo. *Br. J. Haematol.* **1982**, *50*, 575–582. [[CrossRef](#)]

39. Le Jeune, S.; Sadoudi, S.; Charue, D.; Abid, S.; Guigner, J.-M.; Helley, D.; Bihan, H.; Baudry, C.; Lelong, H.; Mirault, T.; et al. Low grade intravascular hemolysis associates with peripheral nerve injury in type 2 diabetes. *PLoS ONE* **2022**, *17*, e0275337. [[CrossRef](#)]
40. Effenberger-Neidnicht, K.; Hartmann, M. Mechanisms of Hemolysis During Sepsis. *Inflammation* **2018**, *41*, 1569–1581. [[CrossRef](#)]
41. Kato, G.J.; Steinberg, M.H.; Gladwin, M.T. Intravascular hemolysis and the pathophysiology of sickle cell disease. *J. Clin. Investig.* **2017**, *127*, 750–760. [[CrossRef](#)] [[PubMed](#)]
42. De Franceschi, L.; Turrini, F.; Honczarenko, M.; Ayi, K.; Rivera, A.; Fleming, M.D.; Law, T.; Mannu, F.; A Kuypers, F.; Bast, A.; et al. In vivo reduction of erythrocyte oxidant stress in a murine model of beta-thalassemia. *Haematologica* **2004**, *89*, 1287–1298. [[PubMed](#)]
43. Bódi, N.; Chandrakumar, L.; al Doghmi, A.; Mezei, D.; Szalai, Z.; Barta, B.P.; Balázs, J.; Bagyánszki, M. Intestinal Region-Specific and Layer-Dependent Induction of TNF α in Rats with Streptozotocin-Induced Diabetes and after Insulin Replacement. *Cells* **2021**, *10*, 2410. [[CrossRef](#)] [[PubMed](#)]
44. Bódi, N.; Mezei, D.; Chakraborty, P.; Szalai, Z.; Barta, B.P.; Balázs, J.; Rázga, Z.; Hermes, E.; Bagyánszki, M. Diabetes-related intestinal region-specific thickening of ganglionic basement membrane and regionally decreased matrix metalloproteinase 9 expression in myenteric ganglia. *World J. Diabetes* **2021**, *12*, 658–672. [[CrossRef](#)] [[PubMed](#)]
45. Barta, B.P.; Onhausz, B.; AL Doghmi, A.; Szalai, Z.; Balázs, J.; Bagyánszki, M.; Bódi, N. Gut region-specific TNFR expression: TNFR2 is more affected than TNFR1 in duodenal myenteric ganglia of diabetic rats. *World J. Diabetes* **2023**, *14*, 48–61. [[CrossRef](#)]
46. Dhaliwal, G.; Cornett, P.A.; Tierney, L.M., Jr. Hemolytic anemia. *Am. Fam. Physician* **2004**, *69*, 2599–2606.
47. Ferreira, J.L.; Gómez-Hospital, J.A.; Angiolillo, D.J. Review article: Platelet abnormalities in diabetes mellitus. *Diabetes Vasc. Dis. Res.* **2010**, *7*, 251–259. [[CrossRef](#)]
48. Scridon, A.; Perian, M.; Marginean, A.; Vantu, A.; Ghertescu, D.; Fisca, C.; Halatiu, V.; Grigoras, T.; Serban, R.C. Streptozotocin-Induced Diabetes Mellitus—A Paradox of High Intrinsic Platelet Reactivity and Low In Vitro Platelet Aggregation. *Acta Endocrinol.* **2019**, *15*, 46–51. [[CrossRef](#)]
49. Waggiallah, H.; Alzohairy, M. The effect of oxidative stress on human red cells glutathione peroxidase, glutathione reductase level, and prevalence of anemia among diabetics. *N. Am. J. Med. Sci.* **2011**, *3*, 344–347. [[CrossRef](#)]
50. Dincer, Y.; Akcay, T.; Alademir, Z.; Ilkova, H. Effect of oxidative stress on glutathione pathway in red blood cells from patients with insulin-dependent diabetes mellitus. *Metabolism* **2002**, *51*, 1360–1362. [[CrossRef](#)]

Disclaimer/Publisher’s Note: The statements, opinions and data contained in all publications are solely those of the individual author(s) and contributor(s) and not of MDPI and/or the editor(s). MDPI and/or the editor(s) disclaim responsibility for any injury to people or property resulting from any ideas, methods, instructions or products referred to in the content.